American Journal of Chemistry 2016, 6(2): 47-54
DOI: 10.5923/j.chemistry.20160602.04

Adsorption of Methylene Blue on the $Li_3Fe_{1-x}Cr_x(MoO_4)_3$ (x = 0, 0.5, 1) Lyonsite Phases

Khadija Gourai[1,*], Abdeslam El Bouari[1], Bouchra Belhorma[2], Lahcen Bih[3]

[1]Department of Chemistry, Laboratory of Physical Chemistry of Applied Materials, Faculty of Sciences Ben M'Sik, University Hassan II Casablanca, Casablanca, Morocco
[2]National Center for Energy, Nuclear Science and Technology, Rabat, Morocco
[3]Team Physical Chemistry of Condensed Matter, Faculty of Sciences Meknes, University Moulay Ismail, Meknes, Morocco

Abstract This work focuses on the study of the adsorption of methylene blue (MB) onto the mixed transition metal oxide compounds $Li_3Fe_{1-x}Cr_x(MoO_4)_3$ (x = 0, 0.5 and 1) of Lyonsite structure. The studies are carried out in "batch methods", and they allowed determining several parameters that govern this adsorption. The influence of pH, temperature, contact time and mass of the adsorbent on the MB adsorption were determined. The adsorption kinetics was analyzed using the Langmuir and Freundlich models. The obtained results show that the adsorption of methylene blue onto these mixed oxides is well described by the model of Langmuir and its kinetic corresponds to the second order.

Keywords Adsorption, Methylene blue, Kinetic, Isotherm, Lyonsite structure

1. Introduction

The treatment of brackish water by reverse osmosis is a membrane filtration technique which allows production of good quality water for different applications (drinking water, agriculture, industries...) [1, 2]. This treatment requires a series of meadows-treatments such as the filtration with activated carbon, which is based on the phenomenon of adsorption, and is relatively easy to implement. The activated carbon is the most widely used adsorbent because of its high adsorption capacity [3]; but it has the disadvantage of a high cost and difficulty to regenerate after each adsorption cycle which limits its commercial application [4]. Hence, several investigations looking for new adsorbents with high efficiency and low cost are performed [5-7]. In order to evaluate how these adsorbents are more effective, the studies considered the investigation of the mechanism of attachment of dye molecules on the surface of the adsorbents.

According to the literature [8, 9], several new adsorbents based on transition metal oxide were proposed. In the framework of looking for new adsorbent materials, our interest is focused on oxide compounds based on molybdate $Li_3Fe_{1-x}Cr_x(MoO_4)_3$ (x = 0, 0.5 and 1) containing transition metals like iron and chromium. In fact, the presence of these transition metals in the structure of these molybdates could facilitate the adsorption and therefore the elimination of impurities from water. The first molybdate material which has the lyonsite structure is the compound $NaCo_{2.31}(MoO_4)_3$ [10]. In general, oxides of lyonsite structure can be expressed as $A_{16}B_{12}O_{48}$ and are composed of an assembly of octahedra AO_6 and tetrahedrons BO_4. The octahedral sites AO_6 are occupied by heavily loaded cations of electrical-charge +5 and +6 and the tetrahedral sites BO_4 are occupied by the cations of charges +1, +2 and +3 such as (Li^+, K^+, Na^+, Zn^{2+}, Ca^{2+}…) [11].

In this work, we present first the method of preparation of the molybdates $Li_3Fe_{1-x}Cr_x(MoO_4)_3$ (x = 0, 0.5 and 1) and then the studies of adsorption of methylene blue onto these compounds. The influence of pH, temperature, contact time and mass of the adsorbent on the adsorption capacity is studied. The adsorption kinetic is determined using the models of Langmuir and Freundlich.

2. Materials and Methods

2.1. Adsorbent

The adsorbents used in this study are the molybdates Lyonsite type of the formulae $Li_3Fe_{1-x}Cr_x(MoO_4)_3$ (x = 0, 0.5 and 1). The powders of $Li_3Fe_{1-x}Cr_x(MoO_4)_3$ are prepared by the soft combustion method which consists to dissolve in a minimum volume of water a mixture of glycine $(C_2H_5NO_2)_2$ and stoichiometric reagents nitrates ($LiNO_3$), $Fe(NO_3)_3.9H_2O$, $Cr(NO_3)_3.9H_2O$ and $(NH_4)_6Mo_7O_{24}.4H_2O$). These solutions provide highly viscous liquids after dehydration at a temperature of 80°C. Then a heat treatment between 150°C and 200°C allows to obtain powders of

* Corresponding author:
gouraikhadija@yahoo.fr (Khadija Gourai)
Published online at http://journal.sapub.org/chemistry

porous molybdates $Li_3Fe_{1-x}Cr_x(MoO_4)_3$. Finally, these powders were submitted to a final heat treatment at 700°C.

The structural analysis of these samples was carried out by X-ray diffraction (XRD) technique using a Bruker D8 Advance apparatus. The UV-Visible spectra of the solutions are measured by a UV-3100PC spectrophotometer VWR. A pH-meter PHSJ-5 was used for the pH measurements.

2.2. Adsorbate

The adsorbate considered in this work is the 3.7-bis-(dimethylamino) phenazathionium known as the methylene blue which is a cationic dye, and it was synthesized the first time by Heinrich Caro in 1876. Its molecular formula is $C_{16}H_{18}ClN_3S$, with a molar mass equal to 319.852 g/mol and a pH equal to 6.5. The Fig.1 shows the chemical structure of methylene blue.

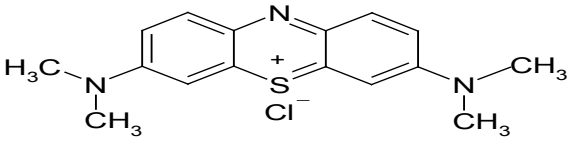

Figure 1. Chemical Structure of methylene blue

2.3. Adsorption Experiments

The adsorption was made in batch method and the concentration of the solution was determined by using UV–visible spectrophotometer (VWR, V 3100). The calculation of the adsorption capacity is carried out from the following equation:

$$Q_e = \frac{(C_0 - C_e)}{m} V \quad (1)$$

where, Q_e: Adsorption capacity of the adsorbent (mg/g), C_0: Initial concentration of dye (mg/l), C_e: Concentration of dye (mg/l) at equilibrium, m: Mass of the adsorbent (g), V: Volume of the solution.

3. Results and Discussion

3.1. X-Ray Diffraction Analysis

X-ray patterns of $Li_3Fe_{1-x}Cr_x(MoO_4)_3$ (x= 0, 0.5 and 1) samples are shown in Fig.2. The replacement of iron (Fe^{3+}) by chromium (Cr^{3+}) gives X-ray patterns with the same shapes but with a small displacement of X-ray peaks. It is demonstrated that the substitution of iron by chromium form a continuous solid solution because Cr^{3+} (r = 0.615 Å) and Fe^{3+} (r = 0.645 Å) [12] have similar sizes. The results show that these materials crystalize in the orthorhombic pattern, with a space group Pnma. The experimental XRD data for all the samples are successfully indexed by DICVOL software and the linear cell parameters are gathered in Table 1. It is noticed that the substitution of iron by chromium induces the decrease of these parameters owing to the fact that the ionic radius of chromium Cr^{3+} is slightly smaller compared to that of Fe^{3+}.

Table 1. Cell parameters of $Li_3Fe_{1-x}Cr_x(MoO_4)_3$ (x = 0, 0.5 and 1) materials

Compound	Lattice parameters		
	a (Å)	b (Å)	c (Å)
$Li_3Fe(MoO_4)_3$	5.123	10.552	17.475
$Li_3Fe_{0.5}Cr_{0.5}(MoO_4)_3$	5.072	10.438	17.423
$Li_3Cr(MoO_4)_3$	5.056	10.344	17.341

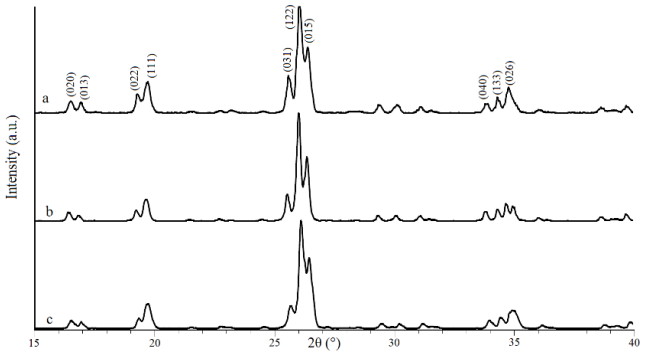

Figure 2. XRD patterns of $Li_3Fe_{1-x}Cr_x(MoO_4)_3$: (a) x = 0, (b) x = 0.5 and (c) x = 1

3.2. Influence of Some Parameters on the Adsorption

3.2.1. Effect of Contact time

The effect of contact time on adsorption of MB onto the $Li_3Fe_{1-x}Cr_x(MoO_4)_3$ (x = 0, 0.5 and 1) samples is studied. The experiments were realized at room temperature by keeping the pH of the solution constant at 6.5 and using 20 mg/l MB. Fig.3 showed the obtained results. The uptake of MB onto the different adsorbents is nearly the same. The adsorption equilibrium is reached in 5 min (28 mg/g), and the adsorption capacity becomes nearly constant without changes after this equilibrium time. The short equilibrium time (5 min) could indicate that the adsorption reaction between MB and lyonsite samples is very fast [13].

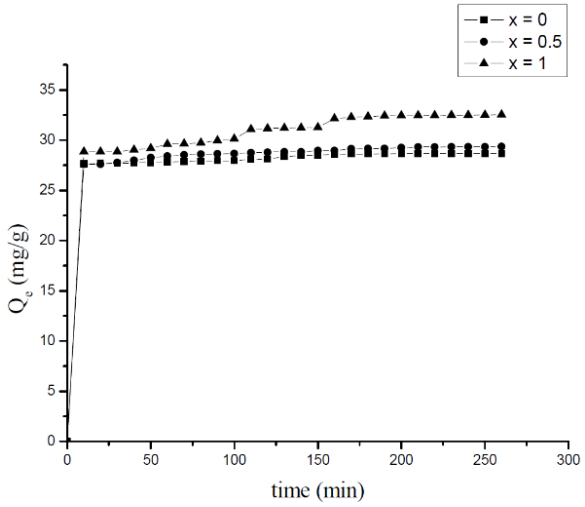

Figure 3. Influence of the contact time on the adsorption of the MB on $Li_3Fe_{1-x}Cr_x(MoO_4)_3$

The substitution of iron by the chromium seems to have a positive effect on the adsorption of MB on the $Li_3Fe_{1-x}Cr_x(MoO_4)_3$ (x = 0, 0.5 and 1) adsorbents. The adsorption capacity increases with the increase of the amount of chromium in the samples. By moving from x = 0 to x = 1 the adsorption capacity increases by a little bit from 27 mg/g to 32 mg/g.

3.2.2. Effect of Temperature

In general, the adsorption depends on the structure of the adsorbent and on the temperature. To get an idea of this dependency, we studied the effect of temperature on the adsorption of MB onto the prepared molybdate adsorbents.

The experiments were performed by adding 20 mg of $Li_3Fe_{1-x}Cr_x(MoO_4)_3$ (x = 0, 0.5 and 1) to a solution of 100 ml of methylene blue at different temperature. The temperatures were set at 25°C, 45°C, 65°C and 75°C using a thermostat bath. Fig.4 shows the dependence of the adsorption content of MB on the temperature.

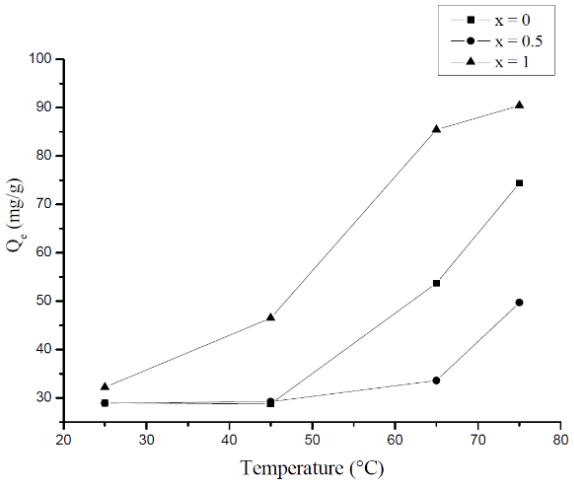

Figure 4. The temperature dependence of the MB adsorption

From Fig.4, one can note that the adsorption capacity increases with the temperature. Actually, from 25°C to 75°C the adsorption capacity of the $Li_3Fe(MoO_4)_3$ increases from 28.944 mg/g to 74.403 mg/g; that of $Li_3Fe_{0.5}Cr_{0.5}(MoO_4)_3$ increases from 28.925 mg/g to 49.726 mg/g; and that of $Li_3Cr(MoO_4)_3$ goes up from 32.184 mg/g to 90.452 mg/g. This induces that the temperature has a positive effect on the adsorption; In fact, the increase of temperature increases the diffusion rate of the adsorbed molecules through particles of the external layer of adsorbent [14]. Moreover, it is showed from the adsorption-temperature dependency that the chromium based compound is more effective for the MB adsorption.

The adsorption process of MB onto the $Li_3Fe_{1-x}Cr_x(MoO_4)_3$ (x = 0, 0.5 and 1) induces some energy changes of the adsorbate-adsorbent system. This energy can be reflected by the thermodynamic parameters such as free energy change (ΔG°, $kJmol^{-1}$), entropy change (ΔS°, $Jmol^{-1}K^{-1}$) and enthalpy change (ΔH°, $kJmol^{-1}$). They can be determined by the following equations:

$$\Delta G = \Delta H - T\Delta S \quad (2)$$

$$\text{Ln } K = \frac{\Delta S}{R} - \frac{\Delta H}{RT} \quad (3)$$

where K is the equilibrium constant.

By plotting LnK as a function of 1/T (Fig.5), we obtained a straight line of slope ΔH/R and the intercept ΔS/R.

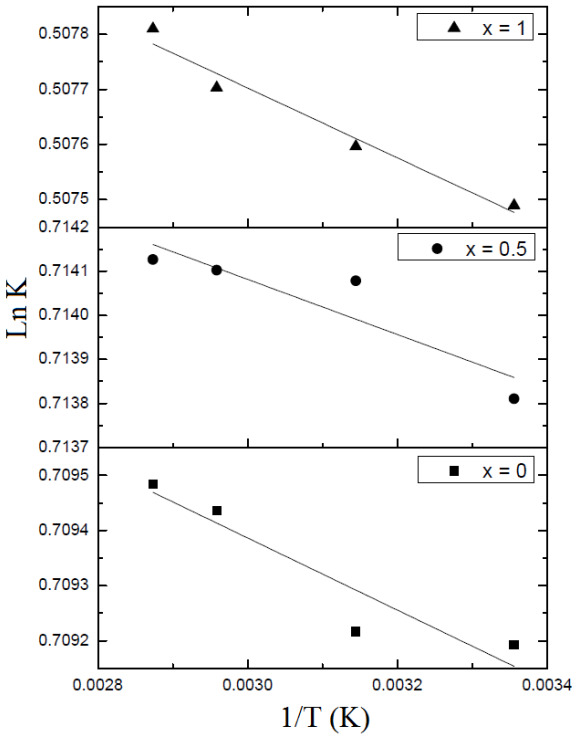

Figure 5. Variation of the equilibrium constant Ln K as a function of temperature for MB adsorption on $Li_3Fe_{1-x}Cr_x(MoO_4)_3$

By determining these thermodynamic parameters one can get more insight to the effect of temperature on the adsorption and investigate the possible mechanism involved in the adsorption process. The calculated values of thermodynamic parameters were gathered in Table 2. It is observed that the free energy values are negative and ascertaining that the adsorption of MB on lyonsite adsorbent is spontaneous and thermodynamically favorable [15]. The mechanism of the adsorption could be understood from the values of the free energy [16]. For instance, it is reported [16] that the change in free energy for physisorption was between -20 and 0 kJ/mol, while chemisorption mechanism was in the range -80 to -400 kJ/mol. According to data of Table 2, the values of (ΔG°) are within the range -20 to 0 kJ/mol. This result suggests the main adsorption of MB onto lyonsite adsorbents could be performed by the physisorption mechanism.

Furthermore, the positive value of ΔH indicated that the adsorption is an endothermic process. In other words, the positive values of the enthalpy energy suggest that the MB adsorption onto the molybdate sorbents is more favorable at high temperatures, in agreement with the dependence of the adsorption with the temperature given in Fig.4. In addition, the positive value of ΔS do indicate the increase randomness

at the solid-solution interface during the adsorption process of MB on the molybdate adsorbents [17]. One can also remark that the given values of the entropy energy are relatively low suggesting that the interactions between MB and the molybdate adsorbents are physical in nature. The same result is proposed elsewhere [18].

Table 2. Thermodynamic parameters of the MB adsorption onto lyonsite $Li_3Fe_{1-x}Cr_x(MoO_4)_3$ adsorbents (x = 0, 0.5 and 1) at various temperatures

		Temperature (K)			
		298	318	338	348
x=0	$\Delta G°(kJ.mol^{-1})$	-0.1407	-0.1502	-0.1596	-0.1643
	$\Delta S°(J.mol^{-1}.K^{-1})$	0.00591	-	-	-
	$\Delta H°(kJ.mol^{-1})$	1.6216	-	-	-
x=0.5	$\Delta G°(kJ.mol^{-1})$	-0.2242	-0.2395	-0.2543	-0.2618
	$\Delta S°(J.mol^{-1}.K^{-1})$	0.00595	-	-	-
	$\Delta H°(kJ.mol^{-1})$	1.5497	-	-	-
x=1	$\Delta G°(kJ.mol^{-1})$	-0.0218	-0.0234	-0.0251	-0.0259
	$\Delta S°(J.mol^{-1}.K^{-1})$	0.00423	-	-	-
	$\Delta H°(kJ.mol^{-1})$	1.0878	-	-	-

3.2.3. Effect of pH

The pH is an important factor in any study of adsorption because it can influence at the same time the adsorbent structure and the mechanism of the adsorption [19]. The effect of the pH on the adsorption is studied by adjusting the initial pH of the methylene blue, by adding NaOH and HCl, to adjust the pH to 2, 4, 6, 8, and 10. The experiments were performed by adding 20 mg of $Li_3Fe_{1-x}Cr_x(MoO_4)_3$ (x = 0, 0.5 and 1) to 100 ml of the methylene blue solution (20 mg/l) at different pH values under the temperature of 25°C.

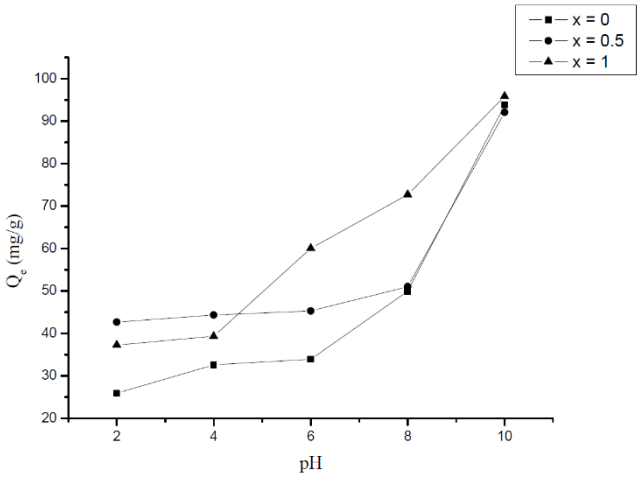

Figure 6. Influence of pH on the adsorption of MB on $Li_3Fe_{1-x}Cr_x(MoO_4)_3$

The effect of the pH of the aqueous solution in the MB adsorption onto the $Li_3Fe_{1-x}Cr_x(MoO_4)_3$ (x = 0, 0.5 and 1) can be attributed to the variation in the degree of ionization of MB and the surface properties of the molybdates. The influence of pH on the adsorption is demonstrated in Fig.6. This latter indicates that an increase in solution pH from 2 to 10 induces an increase in the MB adsorption capacity on molybdate adsorbents. It is observed that the MB adsorption is pH-dependent and the uptake of the MB onto the molybdate adsorbents is favorable at higher pH value. For instance, at low pH values (from 2 to 4), the adsorbed quantity is about 26 mg/g; by increasing pH value up to 6 the uptake quantity becomes 34 mg/g. At high pH values the adsorbed quantity attains 93.8 mg/g [20].

3.2.4. Effect of Adsorbent Mass

The effect of mass is studied by adding 100 ml of 20 mg/l MB to different masses of the lyonsite adsorbent 20, 40, 60, 80 and 100 mg. The experiment is done at room temperature at pH = 6.5. Fig.7 shows the effect of adsorbent mass on MB adsorption by molybdate lyonsite adsorbent.

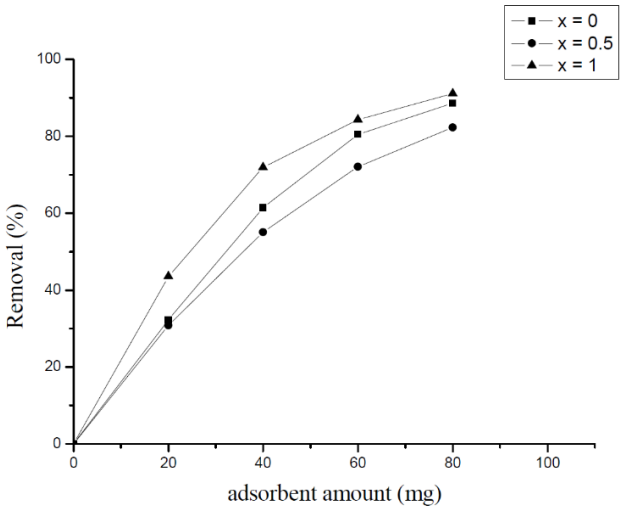

Figure 7. Effect of adsorbent mass on MB adsorption onto $Li_3Fe_{1-x}Cr_x(MoO_4)_3$ phases

The effect of adsorbent mass shown in Fig.7 shows that the increase in adsorbent mass increases the removal rate of MB in the solution. The reason for such behavior could be due to large number of vacant adsorption sites allowing more interactions between MB and molybdate species. This increase of the MB adsorption could also be in favor of the discoloring phenomenon of some aqueous solutions [21]. Furthermore, for the same adsorbent mass, the adsorbent based on chromium molybdate shows high adsorptive reaction of MB in comparison to the other molybdates.

According to the experimental results, it seems that the statistical distributions of chromium and iron in the structure of $Li_3Fe_{1-x}Cr_x(MoO_4)_3$ have an important effect on the MB adsorption. Indeed, in the compounds relatives to pure chromium (x=1) and in its homologous iron molybdate (x=0) in which the distribution of cationic ions is ordered one can observe that the removal rate of MB is high. However, when there is a mixture of cations in the structure (x=0.5) the removal of MB decreases.

3.3. Adsorption Kinetics

The adsorption kinetic is an essential issue in the adsorption studies since it reveals some aspects of the

adsorption process. The study of adsorption kinetics of MB onto $Li_3Fe_{1-x}Cr_x(MoO_4)_3$ (x = 0, 0.5 and 1) molybdates is considered in the framework of the first-order and the second-order models. The conformity between the experimental data obtained from the kinetic experiments and the model prediction are based on the values of the correlation coefficients (R^2); the value of R^2 nearest to the unit indicates the proper model to describe correctly the adsorption kinetics.

The linear forms of these models are given by the following equations:

$$\log(Q_e - Q_t) = \log(Q_e) - \frac{k_1}{2.303}t \quad (4)$$

$$\frac{t}{Q_t} = \frac{1}{k_2 Q_e^2} + \frac{t}{Q_e} \quad (5)$$

where Q_e: Quantity of MB at equilibrium (mg/g), Q_t: Quantity of MB adsorbed at any time t, k_1 (min^{-1}) and k_2 ($g.mg^{-1}.min^{-1}$): the pseudo-first-order and pseudo-order model rate constants, respectively.

The plot of log (Q_e-Q_t) versus time as experimental data is represented in Fig.8. They are fitted by the kinetic model of the pseudo-first order. The correlation coefficient (R^2), k_1 and calculated Q_e are gathered in Table 3. The experimental results fitted by the pseudo-second order model are shown in Fig.9. The amount adsorbed at equilibrium Q_e and the constant of the pseudo-second order k_2 can be determined from the slope and intercept of t/Q_t as function of t. Table 4 summarizes the obtained parameters.

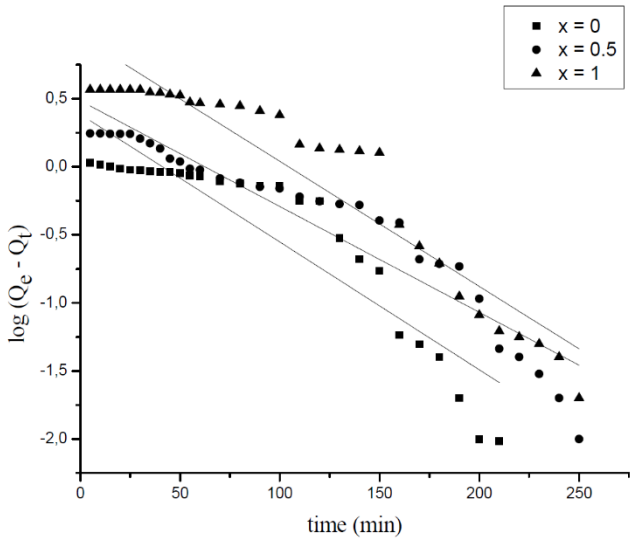

Figure 8. The plots of log (Q_e-Q_t) versus time relative to MB adsorption onto $Li_3Fe_{1-x}Cr_x(MoO_4)_3$

Table 3. The first-order model parameters for MB adsorption on molybdate adsorbents $Li_3Fe_{1-x}Cr_x(MoO_4)_3$

	K^1 (min^{-1})	Q_e ($mg.g^{-1}$) calculated	R^2	Q_e ($mg.g^{-1}$) experimental
x=0	0.027	2.43	0.834	28.66
x=0.5	0.018	3.05	0.899	29.35
x=1	0.021	9.08	0.899	32.53

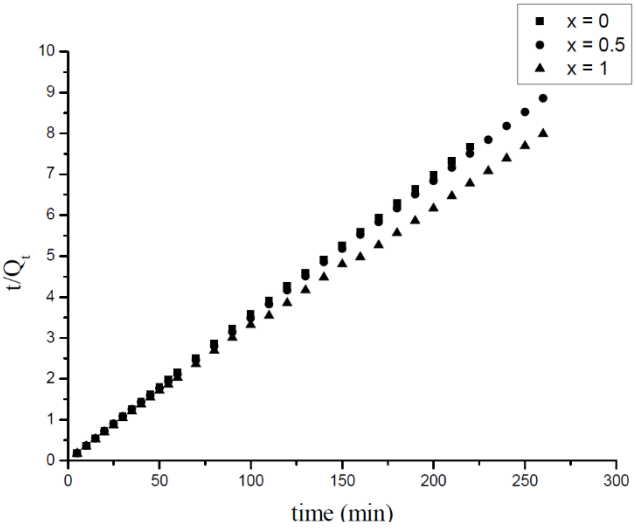

Figure 9. The second order model fits to the experimental data for the adsorption of the MB on $Li_3Fe_{1-x}Cr_x(MoO_4)_3$

Table 4. Parameters of the second order kinetic model for MB adsorption on molybdate adsorbents $Li_3Fe_{1-x}Cr_x(MoO_4)_3$

	Q_e ($mg.g^{-1}$) calculated	K_2 ($mg.g^{-1}min^{-1}$)	R^2	Qe ($mg.g^{-1}$) experimental
x=0	28.73	0.023	0.9999	28.66
x=0.5	29.49	0.017	0.9999	29.35
x=1	33.11	5.5510^{-3}	0.9992	32.53

The calculated (Q_e) of the pseudo-first order model is within the range from 2 to 9 mg/g and the coefficient correlation (R^2) varies from 0.83 to 0.89. On the contrary, the calculated (Q_e) of the pseudo-second order varies according to the chemical composition of the molybdate compounds from 28.73 to 33.11 (mg/g); and the correlation coefficient (R^2) is 0.99. One can note that the correlation coefficient R^2 is very close to the unit while the adsorbed quantity at equilibrium is close to that calculated by employing the pseudo-second order model. This result shows that the second order model fits well the experimental data. According to this kinetic model, the adsorption process under study depends on MB and $Li_3Fe_{1-x}Cr_x(MoO_4)_3$ (x = 0, 0.5 and 1) and the mechanism of the adsorption involves both the chemisorption and/or the physisorption process [22].

3.4. Adsorption Isotherms

Adsorption isotherm describes the relationship between the adsorbed content of one substance and its amount in the equilibrium solution at fixed temperature. It facilitates the description of the interaction between the adsorbate and the adsorbent. Adsorption isotherm represents the amount of the adsorbate bounded to the surface (Q_e) as a function of the material present in the solution (C_e). Fig.10 reproduces the adsorption isotherms relatives to the molybdates $Li_3Fe_{1-x}Cr_x(MoO_4)_3$ (x = 0, 0.5 and 1).

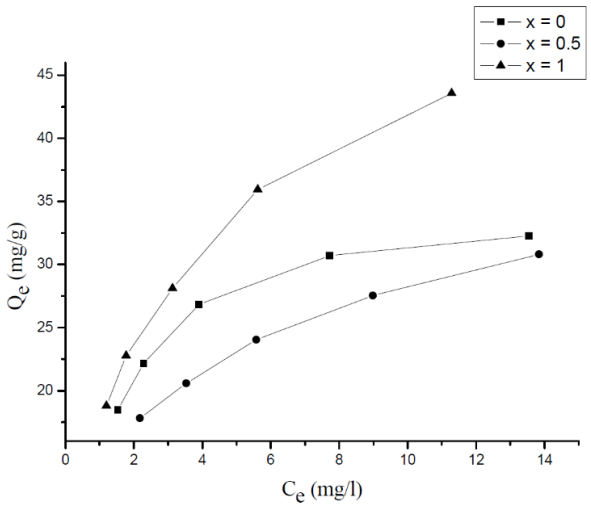

Figure 10. Adsorption isotherm of MB onto $Li_3Fe_{1-x}Cr_x(MoO_4)_3$

According to Giles et al [23], the obtained adsorption equilibrium for MB onto $Li_3Fe_{1-x}Cr_x(MoO_4)_3$ (x = 0, 0.5 and 1) adsorbents belongs to class L curve. It reveals that the MB adsorption process could occur in monolayer form.

In this study two isotherm models namely Langmuir and Freundlich were used to determine the adsorption mechanism of MB onto $Li_3Fe_{1-x}Cr_x(MoO_4)_3$ (x = 0, 0.5 and 1) and the surface properties of the adsorbent.

The Langmuir equation is adapted to describe the behavior of adsorption of homogeneous surfaces. The linear transformation of this model gives the following equation:

$$\frac{1}{Q_e} = \frac{1}{Q_m} + \frac{1}{K_l.Q_m} * \frac{1}{C_e} \quad (6)$$

where Q_e: is the adsorption capacity at equilibrium (mg/g), Q_m: is the maximum adsorption capacity (mg/g), K_l : is the Langmuir equilibrium constant (l/mg) and C_e: is the equilibrium concentration of MB in solution (mg/L).

An essential parameter of the Langmuir isotherm is the parameter R_L; it's defined by the following equation:

$$R_L = \frac{1}{1 + K_l C_0} \quad (7)$$

where K_l is the Langmuir constant and C_0 is the highest adsorbate concentration. When R_L is greater than 1, the adsorption is unfavorable, and when R_L is equal to 1 it indicates that the adsorption is linear, whereas when R_L is between 0 and 1, the adsorption is favorable [24].

On the other hand, the Freundlich model is an empirical expression which assumed that a multilayer adsorption occurs on the heterogeneous surface or surface supporting sites of various affinities. The isotherm is given by the following equation:

$$Q_e = K_f C_e^{1/n_f} \quad (8)$$

where Q_e: is the equilibrium MB concentration on the adsorbent (mg/g), C_e: is the equilibrium concentration of MB in the solution (mg/l), K_f: is the empirical constant of Freundlich isotherm, n_f: is the empirical parameter related to the favorability of the adsorption process. For instance, when the ratio ($1/n_f$) takes values below 1, the adsorption is favorable. The linear form of the equation (8) is the following equation:

$$\text{Ln } Q_e = \text{Ln } K_f + \frac{1}{n_f} \text{Ln} C_e \quad (9)$$

Fig.11 and Fig.12 give the adsorption isotherms of MB onto $Li_3Fe_{1-x}Cr_x(MoO_4)_3$ (x = 0, 0.5 and 1) according to Langmuir and Freundlich models, respectively. Table 5 gathers all the extracted parameters from the used models.

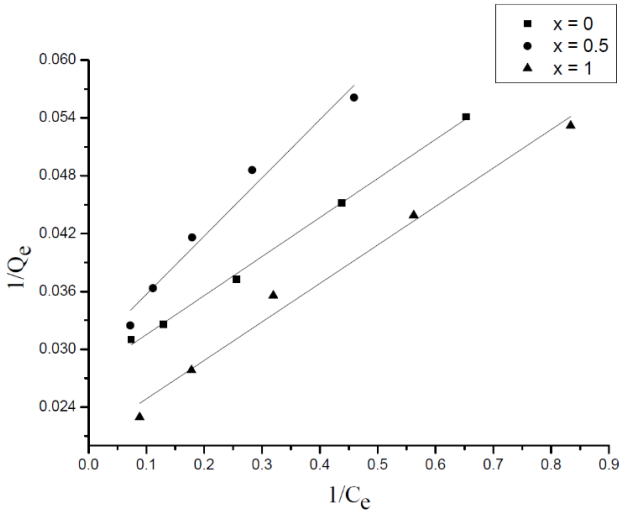

Figure 11. Langmuir isotherm of the MB adsorption onto $Li_3Fe_{1-x}Cr_x(MoO_4)_3$

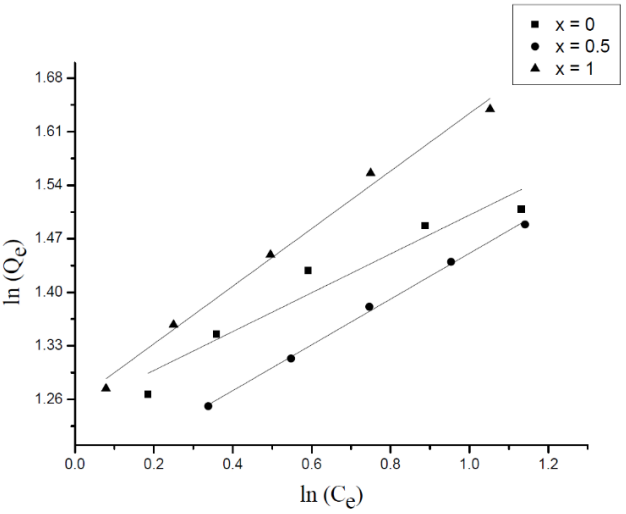

Figure 12. Freundlich isotherm of the MB adsorption onto $Li_3Fe_{1-x}Cr_x(MoO_4)_3$

Table 5. Isotherm parameters and correlation coefficients for the MB adsorption onto $Li_3Fe_{1-x}Cr_x(MoO_4)_3$

	Langmuir Parameters				Freundlich Parameters		
	K_l (1/mg)	Q_m (mg/g)	R^2	R_L	K_f (1/kg)	$1/n_f$	R^2
x=0	0.68	36.36	0.9981	0.07	3.48	3.93	0.9343
x=0.5	0.49	33.67	0.976	0.09~0.1	3.16	3.34	0.998
x=1	0.52	48.07	0.9879	0.09~0.1	3.16	2.67	0.992

The inspection of the data from Table 5 shows that the obtained values for the Langmuir R_L parameter are comprised between 0 and 1, suggesting that the adsorption is favorable. Indeed, the correlation coefficient (R^2) for Langmuir model is high and indicates that the Langmuir model fits well the adsorption of the MB on $Li_3Fe_{1-x}Cr_x(MoO_4)_3$ (x = 0, 0.5 and 1) samples with Q_m= 48.07 for the composition (x=1). This indicates that the adsorption of MB occurs on localized sites with no interaction between MB molecules and that the maximum adsorption occurs when the surface is covered by a monolayer of adsorbate [25]. On the other hand, according to the data of Table 5 and specially the values of the correlation coefficient (R^2) extracted from the fits of the experimental adsorptions by the Freundlich model, one can also consider that the later model could describe the MB adsorption. However, this assumption is rejected since the values of ($1/n_f$) parameter are higher than 1 which makes the adsorption unfavorable.

4. Conclusions

The molybdates $Li_3Fe_{1-x}Cr_x(MoO_4)_3$ (x = 0, 0.5 and 1) have been successfully synthesized by the soft combustion method and proved to belong to the Lyonsite type structure. The adsorption studies showed that these materials can interact with the MB dyes. The results showed that the MB adsorption depended on pH of solution, temperature, adsorbent amount and contact time. The adsorption was found to be favorable with the increasing of pH of solution and it was indicated that the adsorption is more favorable at high temperature. The adsorption of MB onto $Li_3Fe_{1-x}Cr_x(MoO_4)_3$ (x = 0, 0.5 and 1) was best described by the pseudo-second order model. The thermodynamic parameters of the adsorption showed that the adsorption of MB onto $Li_3Fe_{1-x}Cr_x(MoO_4)_3$ (x = 0, 0.5 and 1) is an endothermic process and the interaction between MB and the molybdate adsorbents are physical in nature. The maximum value of the adsorption capacity calculated according to the Langmuir model for the composition (x=1) is 48.07 mg/g. It is also shown that the adsorption is very fast and the substitution of iron by the chromium has a positive effect on the adsorption.

ACKNOWLEDGEMENTS

The authors acknowledge the Institute for Research in Solar Energy and New Energies (IRESEN) for the financial support.

REFERENCES

[1] A. Perez-Gonzalez, A.M. Urtiaga, R. Ibanez, I. Ortiz, 2012, State of the art and review on the treatment technologies of water reverse osmosis cencentrates. Water Research, 46, 267-283.

[2] Mingheng Li, 2012, Optimal plant operation of brackish water reverse osmosis (BWRO) desalination, Desalination, 293, 61-68.

[3] Shaobin Wang, Z.H. Zhu, Anthony Coomes, F. Haghseresht, G.Q. Lu, 2005, The physical and surface chemical characteristics of activated carbons and the adsorption of methylene blue from wastewater, Journal of Colloid and Interface Science, 284, 440-446.

[4] Mohamad Amran Mohd Salleh, Dalia Khalid Mahmoud, Wan Azlina Wan Abdul Karim, Azni Idris, 2011, Cationic and anionic dye adsorption by agricultural solid wates: A comprehensive review, Desalination, 280, 1-13.

[5] A. Santhana Krishna Kumar, Revathi Ramachandran, S. Kalidhasan, Vidya Rajesh, N. Rajesh, 2012, Potential application of dodecylamine modified sodium montmorillonite as an effective adsorbent for hexavalent chromium, Chemical Engineering Journal, 211-212, 396-405.

[6] M. Auta, B.H. Hameed, 2014, Chitosan-clay composite as highly effective and low-cost adsorbent for batch and fixed-bed adsorption of methylene blue, Chemical Engineering Journal, 237, 352-361.

[7] Yanhui Li, Qiuju Du, Tonghao Liu, Jiankun Sun, Yonghao Wang, Shaoling Wu, Zonghua Wang, Yanzhi Xia, Linhua Xia, 2013, Methylene blue adsorption on graphene oxide/calcium alginate composites, Carbohydrate Polymers, 95, 501-507.

[8] Madhumita Bhaumik, Katlego Setshedi, Arjun Maity, Maurice S. Onyango, 2013, Chromium (VI) removel from water using fixed bed column of polypyrrole/Fe_3O_4 nanocomposite, Separation and Purification Technology, 110, 11-19.

[9] K. Miyajima, C. Noubactep, 2012, Effects of mixing granular iron with sand on the efficiency of methylene blue discoloration, Chemical Engineering Journal, 200-202, 433-438.

[10] J. A. Ibers, G.W. Smith, 1964, Crystal structure of a sodium cobalt molybdate, ActaCrystallographica, 17, 190-197.

[11] Jared P. Smit, Peter C. Stair, and Kenneth R. Poeppelmeier, 2006, The adaptable lyonsite structure, Chemistry-A. European J, 12, 5944-4943.

[12] R. D. SHANNON, 1976, Revised Effective Ionic Radii and Systematic Studies of Interatomie Distances in Halides and Chaleogenides, Acta Cryst, A32, 751.

[13] Zhiming Sun, Xiaosuo Qu, Gaofeng Wang, Shuilin Zheng, Ray L. Frost, 2015, Removal characteristics of ammonium nitrogen from wastewater by modified Ca-bentonites, Applied Clay Science 107, 46–51.

[14] Mehmet Dogan, Mahir Alkan, Aydın Türkyilmaz, Yasemin Özdemir, 2004, Kinetics and mechanism of removal of methylene blue by adsorption onto perlite, Journal of Hazardous Materials B109, 141-148.

[15] Nese Ertugay, Emine Malkoc, 2014, Adsorption Isotherm, Kinetic, and Thermodynamic Studies for Methylene Blue from Aqueous Solution by Needles of Pinus Sylvestris L. Pol. J. Environ. Stud, Vol. 23, No. 6, 1995-2006.

[16] Hao Chen, Jie Zhao, Guoliang Dai, 2011, Silkworm exuviae-A new non-conventional and low-cost adsorbent for removal of methylene blue from aqueous solutions, Journal of Hazardous Materials, 186, 1320–1327.

[17] Zhonghui Chen, Jianan Zhang, Jianwei Fu, Minghuan Wang, Xuzhe Wang, Runping Han, Qun Xu, 2014, Adsorption of methylene blue onto poly(cyclotriphosphazene-co-4,4′-sulfonyldiphenol) nanotubes: kinetics, isotherm and thermodynamics analysis, Journal of Hazardous Materials, S0304-3894, 00239-8.

[18] A. Gürses, S. Karaca, Ç. Dogar, R. Bayrak, M. Açıkyıldız, and M. Yalçın, 2004, Determination of adsorptive properties of clay/water system: methylene blue sorption, Journal of Colloid and Interface Science, 269, 310–314.

[19] Denise Alves Fungaro, Mariza Bruno & Lucas Caetano Grosche, 2009, Adsorption and kinetic studies of methylene blue on zeolite synthesized from fly ash, Desalination and Water Treatment, 2, 231-239.

[20] M. Azharul Islama, A. Benhouria, M. Asif, B.H. Hameed, 2015, Methylene blue adsorption on factory-rejected tea activated carbon prepared by conjunction of hydrothermal carbonization and sodium hydroxide activation processes, Journal of the Taiwan Institute of Chemical Engineers, 000 1-8.

[21] A. Aarfane, A. Salhi, M. El Krati, S. Tahiri, M. Monkade, E.K. Lhadi, M. Bensitel, 2014, Kinetic and thermodynamic study of the adsorption of Red195 and methylene blue dyes on fly ash and bottom ash in aqueous medium, J. Mater. Environ. Sci, 5(6) 1927-1939.

[22] Leila Boumehdi Toumi, Lamia Hamdi, Zineb Salem, Khedidja Allia, 2013, Batch adsorption of methylene blue from aqueous solution by untreated Alfa grass. Desalination and Water Treatment, 1-12.

[23] C.H. Giles, D. Smith, J. (1974) Colloid Interf. Sci. 47 755-76.

[24] Dada, A.O, Olalekan, A.P, Olatunya, A.M., Dada, O, 2012, Langmuir, Freundlich, Temkin and Dubinin-Radushkevich isotherms studies of equilibrium sorption of Zn^{2+} unto phosphoric acid modified rice husk, IOSR Journal of Applied Chemistry (IOSR-JAC), 3 38-45.

[25] Khaled Mahmoudi, Khaled Hosni, Noureddine Hamdi, and Ezzeddine Srasra. (2014) Kinetics and equilibrium studies on removal of methylene blue and methyl orange by adsorption onto activated carbon prepared from date pits-A comparative study. Korean J. Chem. Eng, DOI: 10.1007/s11814-014-021 6-y.